International Journal of Applied Earth Observation and Geoinformation 40 (2015) 11–18

Contents lists available at ScienceDirect

International Journal of Applied Earth Observation and Geoinformation

journal homepage: www.elsevier.com/locate/jag

Improved coastal wetland mapping using very-high 2-meter spatial resolution imagery

Matthew J. McCarthy[a,*], Elizabeth J. Merton[b], Frank E. Muller-Karger[a]

[a] Institute for Marine Remote Sensing, College of Marine Sciences, University of South Florida, 140 7th Ave. South, St. Petersburg, FL 33701, USA
[b] Geospatial Analytics Laboratory, Department of Environmental Science, Policy & Geography, University of South Florida St. Petersburg, 140 7th Ave. South, St. Petersburg, FL 33701, USA

ARTICLE INFO

Article history:
Received 15 January 2015
Accepted 13 March 2015

Keywords:
Wetlands
WorldView-2
Landsat 8 OLI
Tampa Bay
Mangroves

ABSTRACT

Accurate wetland maps are a fundamental requirement for land use management and for wetland restoration planning. Several wetland map products are available today; most of them based on remote sensing images, but their different data sources and mapping methods lead to substantially different estimations of wetland location and extent. We used two very high-resolution (2 m) WorldView-2 satellite images and one (30 m) Landsat 8 Operational Land Imager (OLI) image to assess wetland coverage in two coastal areas of Tampa Bay (Florida): Fort De Soto State Park and Weedon Island Preserve. An initial unsupervised classification derived from WorldView-2 was more accurate at identifying wetlands based on ground truth data collected in the field than the classification derived from Landsat 8 OLI (82% vs. 46% accuracy). The WorldView-2 data was then used to define the parameters of a simple and efficient decision tree with four nodes for a more exacting classification. The criteria for the decision tree were derived by extracting radiance spectra at 1500 separate pixels from the WorldView-2 data within field-validated regions. Results for both study areas showed high accuracy in both wetland (82% at Fort De Soto State Park, and 94% at Weedon Island Preserve) and non-wetland vegetation classes (90% and 83%, respectively). Historical, published land-use maps overestimate wetland surface cover by factors of 2–10 in the study areas. The proposed methods improve speed and efficiency of wetland map production, allow semi-annual monitoring through repeat satellite passes, and improve the accuracy and precision with which wetlands are identified.

© 2015 Elsevier B.V. All rights reserved.

1. Introduction

Wetlands are habitats located along the interface between land and either fresh- or saltwater environments, and are characterized by hydric soils that are flooded regularly (Cowardin et al., 1979; Lunetta and Balogh 1999). They are dominated by emergent, scrub, and forested vegetation. Wetlands are estimated to be worth billions of dollars to commercial and recreational fisheries by providing fish and wildlife habitat and nurseries (Dahl and Stedman, 2013; Ozesmi and Bauer 2002; Turner and Gannon 2014). They offer many other ecosystem services, including nutrient and suspended solid removal, flood protection, erosion control, recreation, aesthetics and other cultural values (Turner and Gannon 2014). The United States Environmental Protection Agency (US EPA) has estimated that the economic value of wetland services for even a single swamp is equivalent to up to $5 million in annual water pollution control costs, and up to $1.5 million in flood control costs (Turner and Gannon 2014). Wetlands provide habitat for wetland-dependent birds, which draw 50 million painters and photographers that contribute more than $10 billion per year to the U.S. economy. Nevertheless, the areal extent of wetlands declined rapidly in the 20th century, primarily as a result of development and pollution (Dahl and Stedman 2013; Raabe et al., 2012). This has led to important restoration efforts in the U.S. and elsewhere, which may conserve habitat biodiversity, and ecosystem services and goods (Nellemann and Corcoran 2010; Ozesmi and Bauer 2002; Rains et al., 2012). Because of their importance, wetlands are the only ecosystem covered by a global treaty, specifically the Ramsar Convention on Wetlands signed in 1971.

Wetland maps provide useful tools for wetland protection and management, including understanding impacts due to climate change or direct anthropogenic use (Rains et al., 2012). Wetland extent and change over time are typically evaluated with the help of synoptic mapping tools including aerial and satellite-derived

* Corresponding author. Tel.: +1 727 553 1186; fax: +1 727 553 1103.
E-mail address: mjm8@mail.usf.edu (M.J. McCarthy).

http://dx.doi.org/10.1016/j.jag.2015.03.011
0303-2434/© 2015 Elsevier B.V. All rights reserved.

photographs and digital imagery (Gianinetto et al., 2014; Raabe et al., 2012; Rains et al., 2012; Rundquist et al., 2001; Steffen et al., 2010; Zhang et al., 2011).

The primary objective of this study was to develop a simple and robust methodology for assessing the extent of wetlands using new, high spatial resolution satellite imagery (~2 m and ~30 m) in specific coastal environments of the Tampa Bay estuary, Florida (USA), and compare the results with existing historical wetlands assessments for these regions. The study area was chosen because of its extensive estuarine and palustrine wetlands, and because these are of high relevance to the ecological health and economic vitality of Tampa Bay. Dominant wetland vegetation in the Tampa Bay watershed (~6550 km^2) includes red, white and black mangroves, and buttonwood.

Several existing wetland maps for the region differ in their estimate of wetland extent and location. For example, the land area classified as wetland in the National Oceanic and Atmospheric Administration (NOAA) Coastal-Change Analysis Program (C-CAP) maps does not match contemporary results from either the National Wetland Inventory (NWI) or the Southwest Florida Water Management District (SWFWMD). C-CAP overestimates the wetland class surface area estimates by a factor of almost three relative to the other two for similar mapping years, with a proportional underestimation of upland forest. The complementarity in error between these classes is likely due to the spectral and spatial mixing of wetland and non-wetland vegetation in the Landsat Thematic Mapper-class images (30 m) used for the analyses. Nevertheless, at least one accuracy validation study estimated that C-CAP wetlands, uplands, and water are classified to an accuracy of 95% (C-CAP, 2013).

2. Methods

2.1. Imagery used

To evaluate the applicability of much higher (order of 2 m per pixel) spatial resolution satellite data now available commercially, we examined two images collected by Digital Globe's WorldView-2 satellite sensors. These data, and wetlands classifications derived from them were compared with wetlands extent estimated with data from the Landsat 8 Operational Land Imager (OLI). These two sensor platforms feature different spatial, spectral and radiometric resolutions. Moreover, imagery from the latter are freely available for download, whereas those of the former are commercially dis-

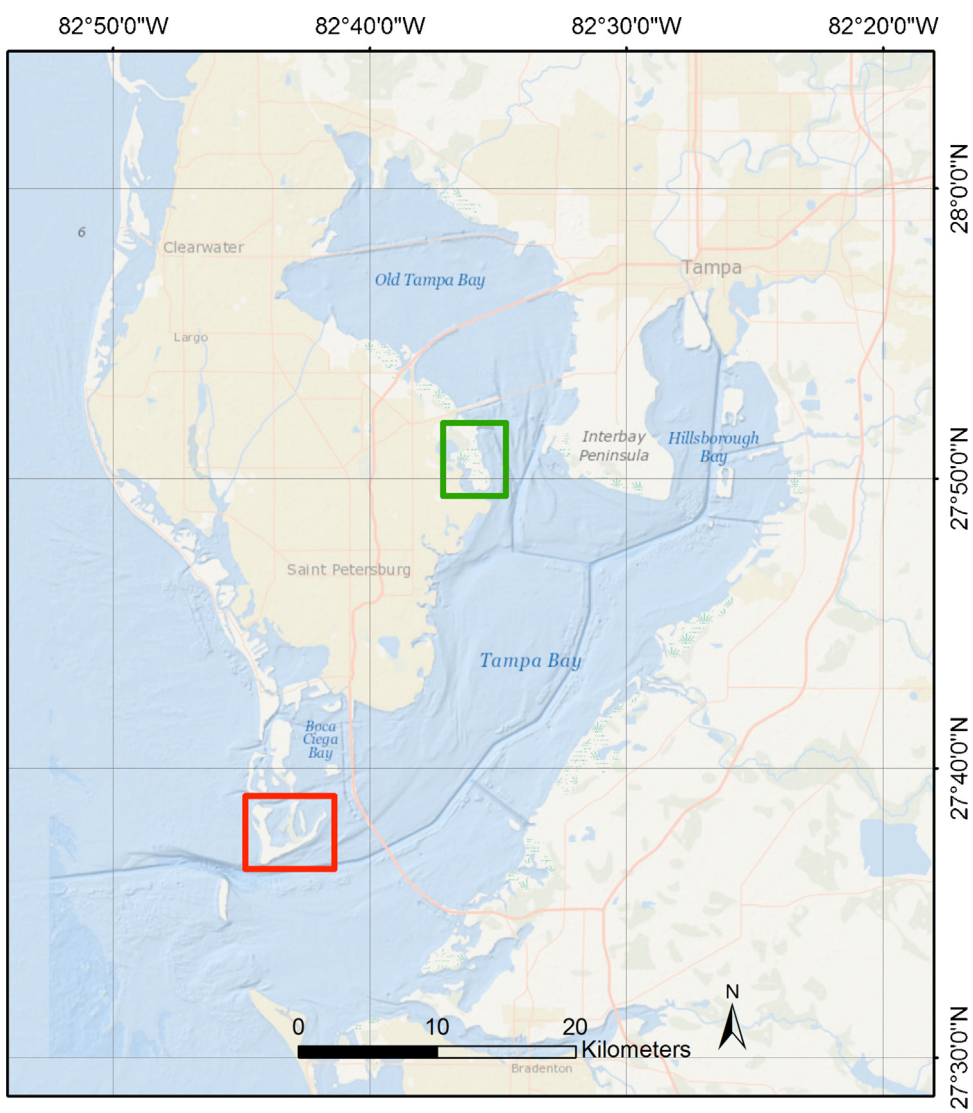

Fig. 1. Study areas in Tampa Bay: Weedon Island (Green box) and Fort De Soto (Red box). (For interpretation of the references to colour in this figure legend, the reader is referred to the web version of this article.)

Table 1
Landsat 8/OLI band specifications.

Band name	Band number	Center wavelength (nm)	Bandwidth (nm)
(Coastal/aerosol)	1	443	433–453
(Blue)	2	482	450–515
(Green)	3	562	525–600
(Red)	4	655	630–680
(NIR)	5	865	845–885
(SWIR 1)	6	1610	1560–1660
(SWIR 2)	7	2200	2100–2300
(PAN)	8	600	500–680
(CIRRUS)	9	1370	1360–1390

tributed – a potentially important factor in deciding which to use for monitoring efforts. We sought to evaluate the differences in the classes derived from these satellite sensors and compare the results with the most recent CCAP, SWFWMD and NWI wetland classes.

Landsat 8 OLI was launched on February 11, 2013. The instrument is a pushbroom system that uses a line of detectors arranged perpendicular to the flight direction collecting images with longer integration times, offering high signal to noise ratios (Vanhellemont and Ruddick, 2014). Imagery is acquired in eight spectral bands, with 12-bit radiometric resolution (Table 1) (Irons et al., 2012).

WorldView-2, launched on October 8, 2009, offers a spatial resolution of about 2 m (Digital Globe 2010). Worldview-2 is the first of the commercial, very high-resolution satellites to provide eight spectral bands in the visible and near-infrared, including coastal and red-edge bands (Table 2) (Digital Globe 2010; Tarantino et al., 2012). WorldView-2 offers an average revisiting time of 1.1 days (Tarantino et al., 2012).

The Landsat 8 OLI image covering both sites was collected in October 12, 2013. The WorldView-2 images were collected in November 8, 2012 (Weedon Island Preserve) and March 7, 2013 (Fort De Soto) (see Fig. 1 for location).

2.2. Study site

Two subregions within Tampa Bay were chosen for this study: Fort De Soto State Park and Weedon Island Preserve (Fig. 1). Fort De Soto is the largest park within the Pinellas County Park System, covering 4.59 km^2. Weedon Island Preserve is even larger at 12.91 km^2. Vegetation at both sites consists of mangroves, wetlands, palm hammocks, hardwoods, and grass flats. Developed land and beach, or barren land, are also prevalent.

2.3. Wetland definition

Wetlands were defined based on the prevalence of four species: *Rhizophora mangle* (red mangrove), *Avicennia germinans* (black mangrove), *Laguncularia racemosa* (white mangrove) and *Conocarpus erectus* (buttonwood). These forested wetlands appear to be frequently misclassified as non-wetland forest. This definition eliminated the need for soils or hydrology data, and allowed for spectral-based identification of the most prevalent wetland species for this area. This differs from the forested wetland definitions used by CCAP, SWFWMD and NWI, which require soil information, a quantification of vegetative cover, or the presence of a vaguely-defined 'hydrophytic vegetation' class.

Table 2
WorldView-2 band specifications.

Band name	Band number	Center wavelength (nm)	Bandwidth (nm)
MS7 (coastal)	1	427	396–458
MS4 (Blue)	2	478	442–515
MS3 (Green)	3	546	506–586
MS6 (Yellow)	4	608	584–632
MS2 (Red)	5	659	624–694
MS5 (Red edge)	6	724	699–749
MS1 (NIR1)	7	833	765–901
MS8 (NIR2)	8	949	856–1043
Panchromatic		627	447–808

2.4. Image pre-processing

Satellite images were radiometrically calibrated by converting digital numbers to radiance values by multiplying the metadata-based gain with the pixel value and adding the offset with ENVI's WorldView Radiance tool (Exelis Visual Information Solutions, Boulder, CO; version 4.5; see Exelis Visual Information Systems, 2014). Pu and Landry (2012) note that atmospheric effects can smear subtle spectral differences between cover types. Yet Harris (2012) confirmed that WorldView-2 radiance images without atmospheric correction are useful to observe objects surrounded by water, and that atmospheric correction of images using Dark Object Subtraction and Fast Line-of-sight Atmospheric Analysis of Hypercubes (FLAASH) markedly decreases the signal to noise ratio of the data. In this study we worked with raw radiances in order to retain any subtle differences in spectra between upland and wetland vegetation.

2.5. Unsupervised classification

A preliminary analysis was conducted to assess the capabilities of the two satellite sensors and determine which was better at identifying wetlands in Fort De Soto using a common, unsupervised classification approach. An unsupervised classification groups together pixels with similar spectral values. It is often used with no previous knowledge of the study area (Lillesand et al., 2008). This classification was first run before any fieldwork was conducted. A normalized difference water index (NDWI) was computed to identify water and exclude it from each image as a mask. Next, the images were segmented into five classes using ENVI's ISODATA unsupervised classification tool. These broad classes were chosen based on existing land cover maps of the area. To identify the land cover type to which each class corresponded, very-high resolution (0.15 m) aerial photographs were used visually as an independent reference. These aerial photographs were collected by the Florida Department of Environmental Protection in 2011 and downloaded from the Land Boundary Information System website (FDEP Land Boundary Information System, 2011). The unsupervised classification corresponded closely to marsh, upland, bare, developed, and grass classes. A second mask was created to exclude bare and developed land from each image. This allowed for the ISODATA algorithm, applied a second time, to distinguish between

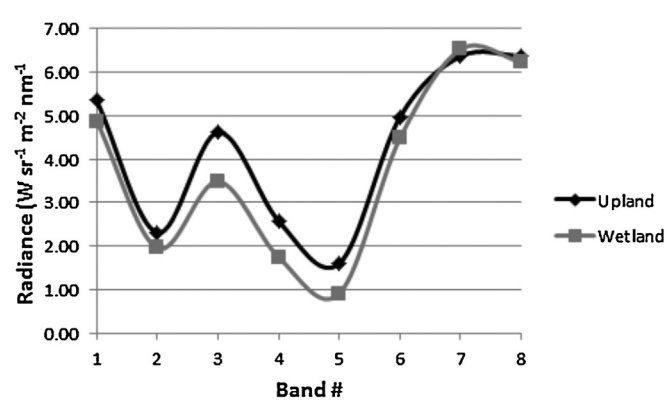

Fig. 2. Plot of average radiance for upland and wetland vegetation based on 780 and 720 spectral profiles, respectively.

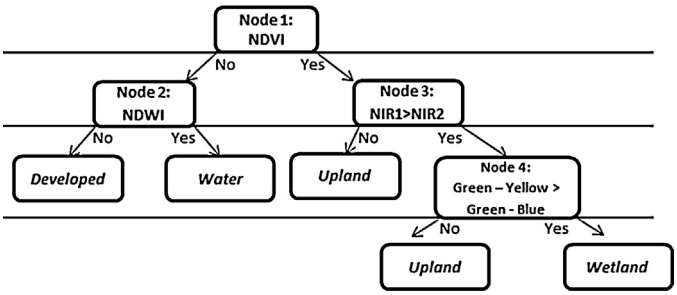

Fig. 3. Decision tree. Bold text indicates a node. Italicized text indicates an identified class.

Table 3
Upland ($n = 780$) and wetland ($n = 720$) radiance ($W\,sr^{-1}\,m^{-2}\,nm^{-1}$) spectral profile assessments combined from both sites. Averages are shown with uncertainties based on one standard deviation.

	Upland	Wetland
Band	Average	Average
1	5.35 ± 0.44	4.88 ± 0.31
2	2.31 ± 0.31	1.95 ± 0.19
3	4.62 ± 0.84	3.49 ± 0.43
4	2.57 ± 0.63	1.74 ± 0.19
5	1.60 ± 0.59	0.91 ± 0.17
6	4.97 ± 1.08	4.48 ± 0.69
7	6.37 ± 1.40	6.53 ± 1.06
8	6.38 ± 1.36	6.24 ± 0.96

vegetation classes. The result was two classified vegetation maps, specifically one from Landsat 8 OLI and one from WorldView-2.

2.6. Field survey

Ground reference points (GRPs) were collected in the field for use in conducting a classification accuracy assessment. We used a Trimble GeoExplorer 6000 series GPS unit (horizontal accuracy of 2.5 cm and vertical accuracy of 4 cm) during May 2014. Habitat classes were identified throughout both study sites where access was feasible. Location was recorded for at least 10 points per class (Barren Land, Developed, Upland, Marsh and Grass). Water was not included in the collection. The points were overlaid on the images using ENVI to confirm congruence with features in the images. All points were separated by at least 20 m to minimize spatial autocorrelation effects (McCarthy and Halls 2014). The GRPs that fit these criteria (55 GRPS for Fort De Soto, 52 for Weedon Island) were then used with ENVI's confusion matrix tool to generate an accuracy assessment for each classified map.

2.7. Decision tree node development and classification

We used a decision tree to conduct classifications. A decision tree is a multi-stage image classifier tool that uses a series of binary decisions to determine the correct class for each image pixel. Each decision node divides the data into one of two classes or groups of classes. No single decision performs the complete segmentation of the image into classes (ENVI Tutorial, 2011). Lu and Weng (2009) found that a decision-tree approach provided an overall accuracy of 92% in land-use classification and that other supervised classification methods yielded lower accuracies. A relatively "mature" classification tool, the decision tree is not a novel approach in itself. Innovative use of one lies in the development of the nodes used to hierarchically identify each pixel's land cover class accurately.

Our decision tree was built to identify 4 land classes: developed/bare, water, upland, and wetland. We were primarily interested in obtaining the highest accuracy of wetlands extent. The results of the unsupervised classification of the WorldView-2 data covering Fort De Soto provided a map of higher accuracy than that of Landsat 8 OLI. The spectral data from the WorldView-2 images were therefore used to define a decision tree based on field-validated locations of specific classes. The decision tree was then used to re-classify the WorldView-2 images of Fort De Soto and Weedon Island.

A normalized difference vegetation index (NDVI) was used in the first node of the decision tree to distinguish vegetated from non-vegetated classes (Eq. (1)) (Wolf 2010). The second Near Infrared band (NIR2, band 8) and the Red band (band 5), centered at 950 and 660 nm, respectively (Table 1), were chosen for this index. In the second node, water was distinguished from developed/bare land using a normalized difference water index (NDWI) (Eq. (2)) using the Coastal band (band 1) and NIR2 (Table 1) (McFeeters 1996).

$$\text{Index} = \frac{(\text{NIR2} - \text{Red})}{(\text{NIR2} + \text{Red})} \tag{1}$$

$$\text{Index} = \frac{(\text{Coastal} - \text{NIR2})}{(\text{Coastal} + \text{NIR2})} \tag{2}$$

Wetland vegetation and upland forest showed similar spectral reflectance patterns (Fig. 2). To identify consistent differences between these vegetation types, 720 wetland and 780 upland spectral profiles from separate pixels were examined for Fort De Soto and Weedon Island field-validated regions. The profiles for both locations were averaged for each class (Table 3 and Fig. 2).

We found that 56% of our collected upland vegetation pixels had maximum radiance values in band 8 (NIR2), whereas 90% of wetland pixels had a maximum in band 7 (NIR1) (Fig. 2; Table 3). These differences in the spectra were used to identify upland vegetation in the third decision-tree node. The difference between band 3 (Green) and band 2 (Blue) radiances was greater for upland in 67% of pixels, and the difference between band 3 (Green) and band 4 (Yellow) radiances was greater for wetland in 96% of pixels. This pattern was used in the fourth and final decision-tree node (Fig. 3) to further distinguish between wetland and upland pixels. These relationships were consistent between the two study sites and for the image acquisition times of March and November.

2.8. Post-processing and accuracy assessment

Classification maps were then filtered using a 3 × 3 pixel median filter in ENVI's Convolutions and Morphology tool to generate more homogenous maps and improve accuracy by replacing isolated cells with the class that corresponds to the median value of cells within a 3 × 3 pixel matrix (McCarthy and Halls, 2014). This is done because habitats tend not to be found in isolation, and isolated pixels are, therefore, likely to be erroneous in classification maps. Accuracy assessment was conducted using ENVI's confusion matrix tool on

Table 4
Confusion matrix results for Fort De Soto (90.9% overall accuracy, Kappa 0.8569).

Class	Producer's accuracy (%)	User's accuracy (%)	Commission error (%)	Omission error (%)
Wetland	81.82	90.00	10.00	18.18
Upland	90.48	90.48	9.52	9.52
Bare/Developed	95.65	91.67	8.33	4.35

Table 5
Confusion matrix results for Weedon Island (84.6% overall accuracy, Kappa 0.7245).

Class	Producer's accuracy (%)	User's accuracy (%)	Commission error (%)	Omission error (%)
Wetland	94.44	77.27	22.73	5.56
Upland	82.76	88.89	11.11	17.24
Bare/Developed	60.00	100.00	0.00	40.00

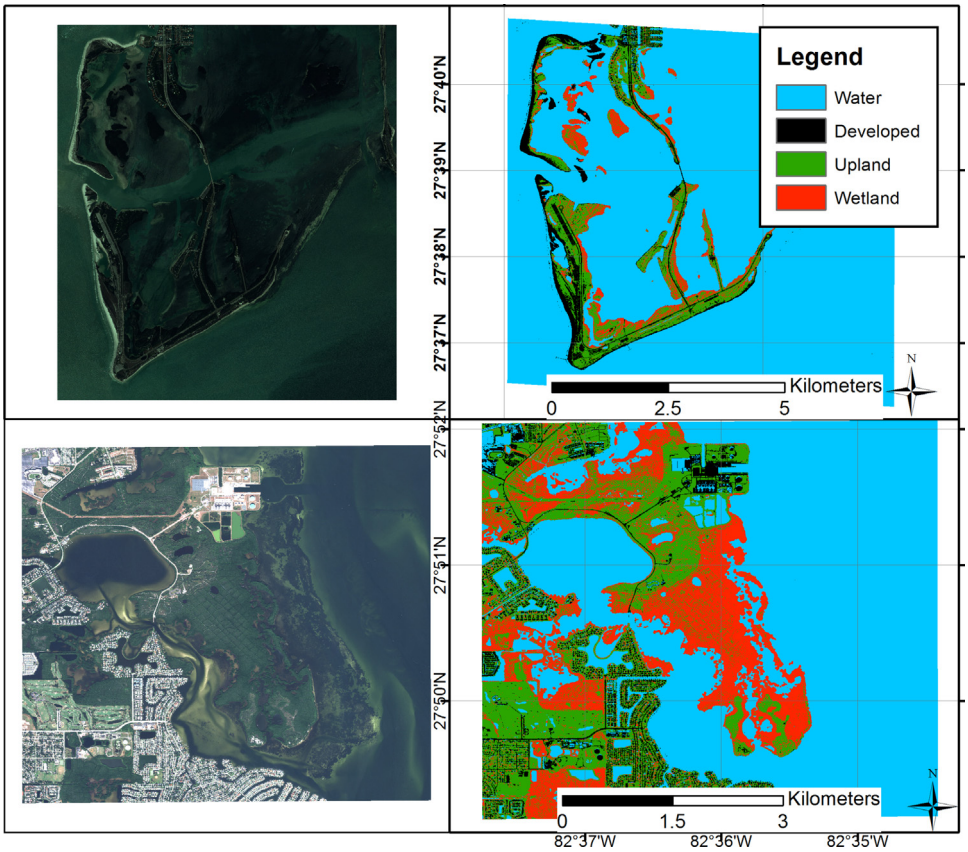

Fig. 4. WorldView-2 image and Decision tree classification maps for Fort De Soto (upper left and right) and Weedon Island (lower left and right).

three classes using the collected GRPs: Wetland, Upland, and Developed/Bare.

3. Results

3.1. Unsupervised classifications

The initial unsupervised classifications of Fort De Soto using WorldView-2 data yielded a Wetland accuracy of 82%, while using Landsat 8 OLI the accuracy was 46%. Upland and Grass accuracies were 67% and 22%, respectively, for WorldView-2, and 58% and 67%, respectively, for Landsat 8 OLI. Because our primary interest was to improve existing wetland maps, we selected WorldView-2 for further analysis to generate the spectral profiles, and train and apply the decision tree.

3.2. Decision tree classifications

The WorldView-2 product derived with the decision tree classification yielded an accuracy (producer's accuracy) of 82% for Wetland in Fort De Soto and 94% in Weedon Island (Tables 4 and 5). Identification of Upland vegetation accuracy was 90% in Fort De Soto and 83% in Weedon Island. User's accuracy for the Wetland class – an index that would be low if wetlands were misclassified as other classes – was 90% for Fort De Soto and 77% for Weedon Island. Producer's accuracy for Developed land was 96% for Fort De Soto and 60% for Weedon Island. None of the Developed-land GRPs were found to be misclassified as Wetland. Decision tree classification maps for each study site are shown with the original images in Fig. 4.

4. Discussion

Remote sensing observations collected at very high spatial resolution, and at high radiometric and spectral resolution, have advanced studies of land use over large areas (Gianinetto et al., 2014). Our study finds that land classification maps derived for two specific coastal habitats within the Tampa Bay estuary using WorldView-2 images had higher accuracy relative to maps derived with Landsat 8 OLI, using ground observations as a reference. In general, the radiometric quality of the Landsat 8 OLI data is comparable to that of the WorldView-2 data (Irons et al., 2012; Tarantino et al., 2012). Also, the spectral resolution of the bands used from each of these sensors is similar (see Tables 1 and 2). Thus, differences in accuracy between the maps derived from the two sensors are likely due to the difference in spatial resolution. Our field evaluations confirmed that many coastal wetland habitats in the two study areas were patchy and often narrow (approximately 5–10 m

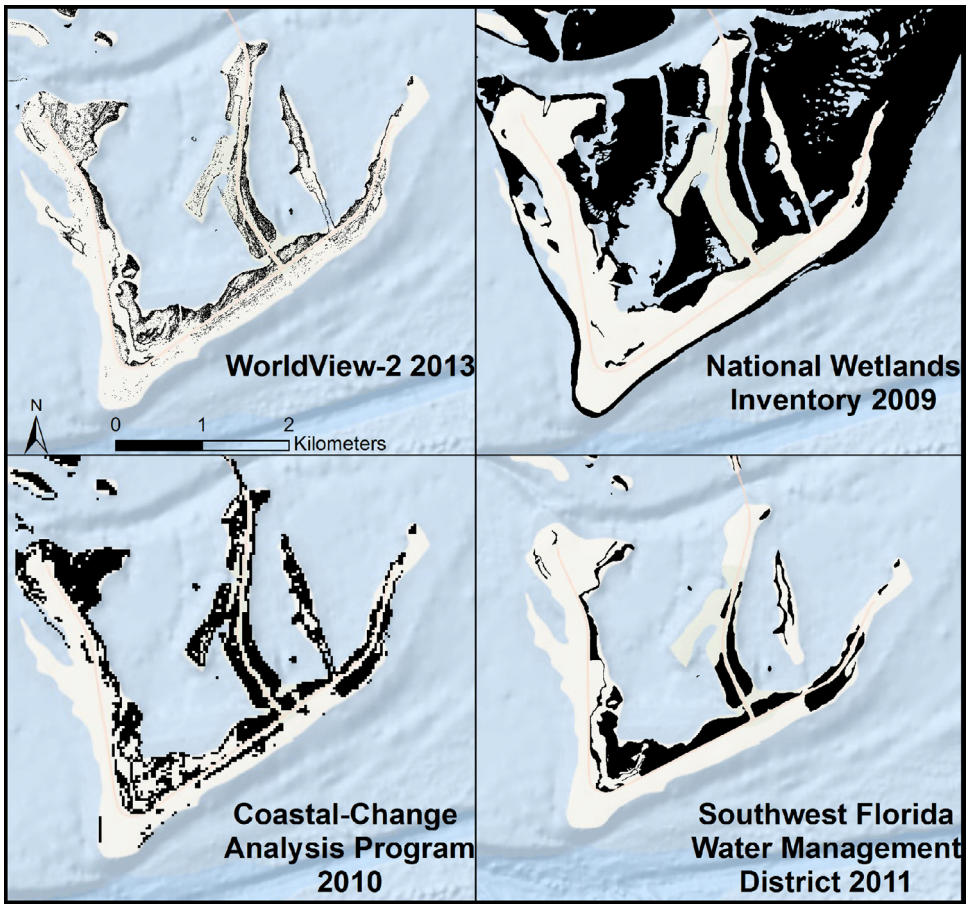

Fig. 5. Wetlands (black) of Fort De Soto from this study (top left) and comparable mapped products with map source and year of remotely sensed data.

wide strips). The 30 m × 30 m pixels of Landsat 8 OLI do not resolve these areas or the mixed vegetation that would be aggregated within each 30 m pixel. In contrast, the very high resolution of WorldView-2 images is able to resolve these vegetation classes (Fig. 5).

One of the goals of this project was to develop a method that could be implemented with relatively minimal resources, and without need for training data. The decision tree tool can be found or created in common image-processing software, and our novel combination of nodes can be copied from this manuscript and applied. We believe that this work has high potential for monitoring in the future when a substantial time series of WorldView-2 imagery is available. Moreover, while we have only validated this approach for the WorldView-2 sensor, it may be applicable to other digital remote sensing data with similar spectral and radiometric resolutions. The decision tree that we developed led to a capability to identify wetland vegetation to greater than 80% accuracy in an objective, automated process using WorldView-2 images. This process did not require ancillary data such as soil or hydrology information. Accurate identification of upland vegetation was also greater than 80%. This process substantially decreased overestimation of wetland area by reducing misclassification of non-wetland vegetation as wetland when compared with other groups' mapped products.

The NIR2 and Yellow bands of the WorldView-2 sensor allowed the segregation of upland and wetland in the decision tree consistently across the two different study areas and in imagery acquired during different seasons. Wang and Sousa (2009) present figures of the mean and standard deviations of mangrove spectral reflectance patterns across visible and near infrared wavelengths for healthy and stressed plants. Variance in reflectance, and differences between spectra of healthy and stressed species, are smaller in the visible wavelengths used in our study than at wavelengths greater than 1000 nm (Wang and Sousa, 2009). Seasonal differences are expected to influence vegetation spectra patterns. Yet Flores-de-Santiago et al. (2012) found no differences in reflectance patterns of healthy or stressed mangrove species in western Mexico along the Gulf of California from the dry to the wet season. The climate in the Tampa Bay area is more moderate than their study area, and the low spectral radiance variation in our wetlands pixels was consistent with that study. We therefore, expect that the spectral patterns of wetlands identified in this study are stable. Future research is needed to validate across greater spatio-temporal ranges the consistent radiance patterns found here.

Benefits of this methodology for future wetland monitoring efforts include further standardization of wetland classification, efficient mapping with a four-node decision tree on digital data, and improved precision of wetland area identification with very high resolution imagery. The implication is that wetlands can now be identified faster and more precisely than before with higher accuracy.

C-CAP, NWI and SWFWMD products used different data and methods for identifying wetlands (C-CAP, 2013; Cowardin et al., 1979; Kawula 2009; National Wetlands Inventory Program, 2014; Southwest Florida Water Management District, 2011). Those products show substantial inconsistencies between wetlands coverage (Figs. 5 and 6). While C-CAP reports an overall accuracy of >80%, large errors were reported in the user's and producer's accuracies for wetland classes (NOAA, 2006). The NWI maps were created by digitizing polygons in a geographic information system using

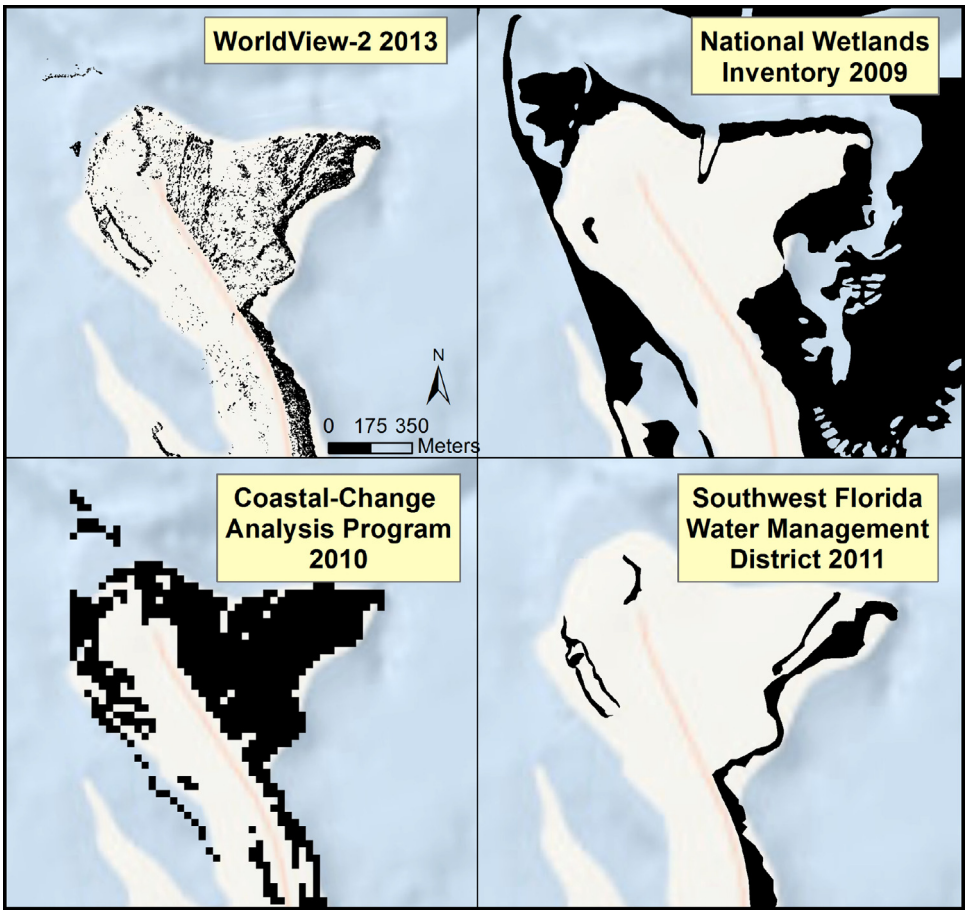

Fig. 6. Wetlands (black) of North Beach subsection of Fort De Soto from this study (top left) and comparable mapped products with map source and year of remotely sensed data.

Table 6
Wetland area computed from map products of Fort De Soto (22 km^2 region of interest), and Weedon Island (27 km^2 region of interest).

	Fort De Soto		Weedon Island	
Map source	Wetland area (km^2)	Factor difference from this study	Wetland area (km^2)	Factor difference from this study
WorldView-2	0.94	N/A	6.17	N/A
SWFWMD	2.49	2.64	8.19	1.33
C-CAP	4.99	5.31	12.74	2.06
NWI	9.92	10.55	12.43	2.01

aerial photographs. The SWFWMD maps were created using a process similar to that used by the NWI (Raabe et al., 2012; Rains et al., 2012). All three products overestimate wetland area relative to our high-resolution WorldView-2 product in both Fort De Soto and Weedon Island (Table 6). The SWFWMD map shows more than double the wetland area, and the CCAP maps report more than five times the wetland area than our product. The ten-fold greater NWI wetland area includes submerged wetlands, which were not considered in the other three maps. We found similar discrepancies for the Weedon Island study area, which includes residential areas of Pinellas County outside the preserve (Table 6).

Given the high accuracy and low misclassification error of this study's wetland maps, we conclude that wetland areas in the C-CAP, NWI and SWFWMD data sets have been overestimated. The latter wetland maps have been used historically to guide restoration efforts in the Tampa Bay watershed (Rains et al., 2012; Robison 2010). We recommend that the methodology used for setting restoration goals be reviewed. It may be appropriate to adopt new methodologies for land classification, such as those used in this study, to establish a more accurate baseline of current wetland area. This would be a better baseline against which to monitor future wetland change.

Additional research is needed to improve the identification of other vegetation types, including forested wetland, scrub-shrub wetland, and emergent wetland. Also, further studies would help to expand the decision tree's capability to identify inland wetlands, which would include distinguishing between palustrine and estuarine wetlands.

6. Conclusions

The goals of this research were to test the applicability of very high spatial resolution (2 m) WorldView-2 satellite observations to quantify wetland area in two regions of interest in the Tampa Bay Florida, USA, watershed. A decision-tree image classification method was used to derive various traditional land and land-use classes. Our methodology identified wetlands with high accuracy and higher precision than previously achieved using satellite and aerial photograph based

data. The decision tree method was rapid and efficient. Our results show that the area of coastal wetland vegetation in our study areas around Tampa Bay is about half that reported in publicly-available products derived from remote sensing methods. Very high resolution WorldView-2 imagery and the decision tree methodology developed here may be useful tools to help focus future monitoring and restoration efforts.

Conflict of interest

The authors declare that they have no conflict of interest.

Acknowledgements

Support for this study was provided by grant to FMK. WorldView-2 images were facilitated by Digital Globe under licensed agreement with the National Science Foundation and were provided by D. Paul Morin of the Polar Geospatial Center, University of Minnesota. The authors thank Tampa Bay Estuary Program employees Lindsay Cross and Ed. Sherwood for their comments in preparation of this work. We also thank Pinellas Country for granting permission to conduct research in Fort De Soto and Weedon Island. Field work was assisted by Lindsey Brendis, Steven Douglas, Jennifer Granneman, Kimberly Lyons, and Devlin Munion. We thank Dr. Barnali Dixon (University of South Florida, St. Petersburg) for her encouragement and advice during this project.

References

C-CAP, 2013. Assessment report of wetland mapping improvement to NOAA's Coastal Change Analysis Program (C-CAP) land cover in western Washington State. State of Washington Department of Ecology. <http://www.ecy.wa.gov/programs/sea/wetlands/pdf/C-CAPWetlandAssessmentReport.pdf/>. (accessed 20.04.14.).

Cowardin, L., Carter, V., Golet, F., LaRoe, E., 1979. Classification of Wetlands and Deepwater Habitats of the United States, FWS/OBS79/31. U.S. Fish and Wildlife Service, Washington.

Dahl, T., Stedman, S., 2013. Status and trends of wetlands in the coastal watersheds of the Conterminous United States 2004 to 2009. U.S. Department of the Interior, Fish and Wildlife Service and National Oceanic and Atmospheric Administration, National Marine Fisheries Service. (46 p.).

Digital Globe, 2010. The Benefits of the Eight Spectral Bands od WorldView-2. Available in <http://www.digitalglobe.com/sites/default/files/DG-8SPECTRAL-WP.pdf/>. (accessed 26.06.14.).

ENVI Tutorial, Decision Tree Classification. <http://www.ittvis.com/language/en-us/productsservices/envi/tutorials.aspx/>. (accessed 15.05.14.).

Exelis Visual Information Systems, 2014. Radiometric Calibration. Calibrating Images Tutorial. <http://www.exelisvis.com/docs/RadiometricCalibration.html/>. (accessed 21.04.14.).

FDEP Land Boundary Information System, 2011. Pinellas [air photo]. 1:6,000. Photo #B089. Brooksville, FL.

Flores-de-Santiago, Kovacs, J.M., Flores-Verdugo, F., 2012. Seasonal changes in leaf chlorophyll *a* content and morphology in a sub-tropical mangrove forest of the Mexican Pacific. Mar. Ecol. Prog. Ser. 444, 57–68.

Gianinetto, M., Rusmini, M., Candiani, G., Via, G.D., Frassy, F., Maianti, P., Marchesi, A., Nodari, F.R., Dini, L., 2014. Hierarchical classification of complex landscape with VHR pan-sharpened satellite data and OBIA techniques. Eur. J. Remote Sens. 47, 229–250.

Harris, T., 2012. Spectral Target Detection for Detecting and Characterizing Floating Marine Debris. American Geophysical Union, San Francisco, CA, Dec. 3–7.

Irons, J.R., Dwyer John, L., Barsi Julia, A., 2012. The next landsat satellite: the landsat data continuity mission. Remote Sens. Environ. 122, 11–21.

Kawula R., 2009. Florida Land Cover Classification System. <http://myfwc.com/media/1205712/SWG%20T-13%20Final%20Rpt_0118pdf/>. (accessed 21.04.14.).

Lillesand, T., Kiefer, R., Chipman, J., 2008. Remote Sensing and Image Interpretation, 6th ed. John Wiley & Sons, Inc., Hoboken, NJ, USA.

Lu, D., Weng, Q., 2009. Extraction of urban impervious surfaces from an IKONOS image. Int. J. Remote Sens. 30, 1297–1311.

Lunetta, R., Balogh, M., 1999. Application of multi-temporal Landsat 5 TM imagery for wetland identification. Photogr. Eng. Remote Sens. 65, 1301–1310.

McCarthy, M.J., Halls, J., 2014. Habitat mapping and change assessment of coastal environments: an examination of WorldView-2, QuickBird, and IKONOS satellite imagery and airborne LiDAR for mapping barrier island habitats. Int. J. Geo-Information 3, 297–325.

McFeeters, S.K., 1996. The use of the normalized difference water index (NDWI) in the delineation of open water features. Int. J. Remote Sens. 17, 1425–1432.

National Wetlands Inventory Program [NWI], 2014. NWI Program Overview. Available in <http://www.fws.gov/wetlands/NWI/Overview.html/>. (accessed 29.05.14.).

Nellemann, C., Corcoran, E., 2010. Dead Planet, Living Planet. Biodiversity and Ecosystem Restoration for Sustainable Development, a Rapid Response Assessment. United Nations Environment Programme, GRID-Arendal, Arendal, Norway, pp. p.109.

NOAA Coastal Change Analysis Program (C-CAP) Land Cover and Change Data [computer file], Charleston, SC: NOAA Coastal Change Analysis Program (C-CAP), 2006. Available at: LAGIC <http://lagic.lsu.edu/data/losco/landcover_la_noaa_2005html#8/>. (accessed 21.04.14.).

Ozesmi, S.L., Bauer, M.E., 2002. Satellite remote sensing of Wetlands. Wetlands Ecol. Manage. 10, 381–402.

Pu, R., Landry, S., 2012. A comparative analysis of high spatial resolution IKONOS and WorldView-2 imagery for mapping urban tree species. Remote Sens. Environ. 124, 516–533.

Raabe, E., Roy, L., McIvor, C., 2012. Tampa Bay coastal wetlands: nineteenth to twentieth century tidal marsh-to-mangrove conversion. Estuaries and Coasts 35, 1145–1162.

Rains, M., Landry, S., Seidel, V., Crisman, T., 2012. Prioritizing habitat restoration goals in the Tampa Bay watershed. Technical report to the Tampa Bay Estuary Program # 10–12. <http://www.tbeptech.org/TBEP_TECH_PUBS/2012/TBEP_10_12_USF_Prioritizing_Habitat_Restoration_Goals_2012_04pdf/>. (accessed 18.05.14.).

Robison, D., 2010. Tampa Bay Estuary Program habitat master plan update. Technical report to the Tampa Bay Estuary Program # 06–09. Available in <http://www.tbeptech.org/TBEP_TECH_PUBS/2009/TBEP_06_09_Habitat_Master_Plan_Update_Report_July_2010pdf/>. (accessed 18.05.14).

Rundquist, D.C., Naraumalani, S., Narayanan, R.M., 2001. A review of wetlands remote sensing and defining new considerations. Remote Sens. Rev. 20 (3), 207–226.

Southwest Florida Water Management District [SWFWMD], 2011. Land Cover Land Use. 2011. <http://www.swfwmd.state.fl.us/data/gis/libraries/physical_dense/lu11php/>. (accessed 29.05.14.).

Steffen, M., Estes, M., Al-Hamdan, M., 2010. Using remote sensing data to evaluate habitat loss in the Mobile, Galveston and Tampa Bay watersheds. Coastal Education and Research Foundation, p.24. <http://weather.msfc.nasa.gov/applied_science/Wetland_Paper_Final.pdf/> (accessed 20.03.14.).

Tarantino, C., Adamo, M., Pasquariello, G., Lovergine, F., Blonda Tomaselli, P.V., 2012. 8-band image data processing of the worldview-2 satellite in a wide area of applications. In: Rustamov, R. (Ed.), Earth Observation., http://dx.doi.org/10.5772/27499, ISBN: 978-953-307-973-8, InTech, Available from: http://www.intechopen.com/books/earth-observation/8-band-image-data-processing-of-the-worldview-2-satellite-in-a-wide-area-of-applications

Turner, M., Gannon, R., 2014. Values of Wetlands. North Carolina State University. <http://www.water.ncsu.edu/watershedss/info/wetlands/values.html/> (accessed 21.04.14.).

Vanhellemont, Q., Ruddick, K., 2014. Turbid wakes associated with offshore turbines observed with Landsat 8. Remote Sens. Environ. 145, 105–115.

Wang, L., Sousa, W.P., 2009. Distinguishing mangrove species with laboratory measurements of hyperspectral leaf reflectance. Int. J. Remote Sens. 30 (5), 1267–1281.

Wolf, A., 2010. Using WorldView-2 Vis-NIR MSI imagery to support land mapping and feature extraction using normalized difference index ratios. Digital Globe: 8-band challenge. Longmont, CO. <http://www.exelisvis.com/portals/0/pdfs/envi/8_bands_Antonio_Wolf.pdf/> (accessed 5.06.14.).

Zhang, Y., Lu, D., Yang, B., Sun, C., Sun, M., 2011. Coastal wetland vegetation classification with a landsat thematic mapper image. Int. J. Remote Sens. 32 (2), 545–561.